

CHAPTER 3

RESULTS AND DISCUSSION

3.1 Direct current conductivity detector with GD-FI system for DIC determination

3.1.1 Characteristic of the fabricated DC Conductivity detector in FI system

The proposed DC conductivity detection approach was performed based on the applying direct potential (pulseless) to the two identical electrodes and as a result, the electrolytic reaction of water was proceeded at the small electrodes and produce a current to flow. The electrolytic reaction of water occurs at both electrodes, both H^+ and OH^- are generated. The presence of some trace inorganic ion in water could make the change of conductivity and as a result enhance the current flow in the electrolytic cell. The electrolytic current is proportional to the concentration of inorganic ion. Consequently, the direct current electrolytic cell could play a role as the conductivity detector for measuring trace concentration of some inorganic ions in water. Normally, the electrolytic reaction of water would produce the hydrogen gas as a gas bubble on the electrode surface, the gas bubble could interrupt the current flowing measurement. But in some experimental condition such as flow condition or stirring solution which the gas bubble can be removed efficiently, the fluctuation of current measuring was ignored and the conductivity signal can be measured [52]. Previously, DC conductivity detector was used for ion chromatography experiment [54]. Although, the true conductance signal cannot be measured from the proposed detector, the change of relative current due to the analyte zone would provide the relative peak signal which corresponding to the salt concentration and available for quantitative chemical analysis.

The peak height signal of DC conductivity detector depends on the applied potential to electrodes [54]. The higher applied potential used, the higher signal can be obtained. But the higher applied voltage would generate higher rate of gas bubble at the

electrode surface. The gas bubble from electrolytic reaction could make the fluctuation of signal and as a result higher standard deviation of baseline (SD_b). In order to evaluate the appropriate applied voltage, the ratio of peak height signal (PS) and standard deviation of the baseline (SD_b) which represent the limit of detection (LOD) in chemical analysis, was defined in this experiment. The PS/SD_b ratio and well-defined peak shape in FI-gram were considered to evaluate the different format of DC conductivity detectors.

The DC conductivity detectors were fabricated in 2 formats as described previously. The first format, as shown a circuit in Figure 3.1, the voltage regulator (7805 or 7815 IC) provides a constant voltage, +5V (or +15V), to the conductivity cell and a constant resistor as potential divider circuit. The output signal voltage correlates to the change of resistance (or reciprocal of conductance) of the conductivity cell as explained in Equation 3.1. The higher concentration of the salt provides the higher conductance of solution, and as a result, the resistance of conductivity cell is less as following Equation 1.3 and it provides the increasing of the output signal as following Equation 3.1.

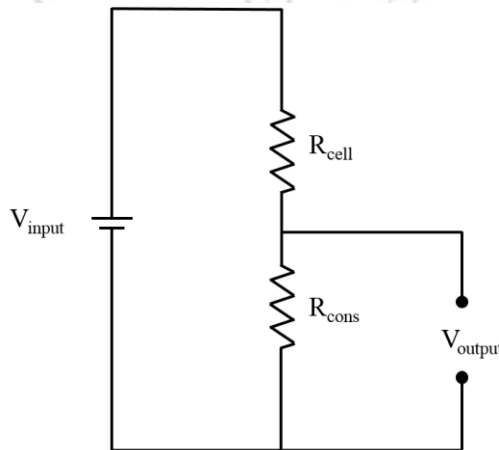


Figure 3.1 Potential divider circuit

$$V_{output} = V_{input} \cdot \frac{R_{cons}}{R_{cons} + R_{cell}} \quad [3.1]$$

The second format, the constant voltages ($\pm 5V$ and $\pm 9V$) were regulated by using 7805/7905 IC were applied to the Wheatstone bridge circuit as shown in Figure 3.2. The output signal was obtained from the different voltage between the two parallel potential divider circuits as explained in Equation 3.2. Then, the FET-input operational amplifier (TL072) was used to differentiate and amplify the voltage signal from the Wheatstone

bridge. From this circuit, the change of resistance in conductivity cell provides the change of output signal.

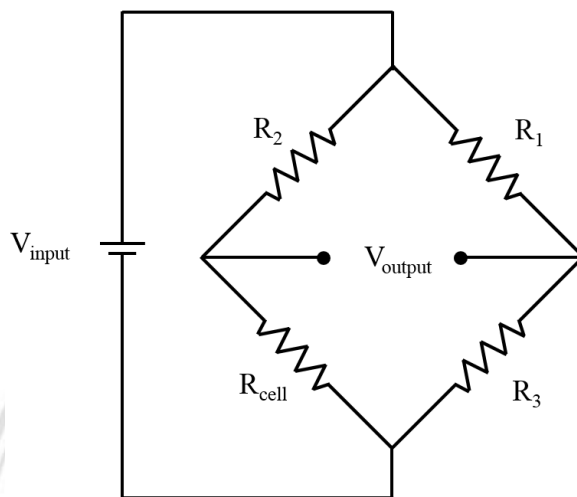


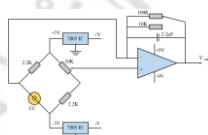
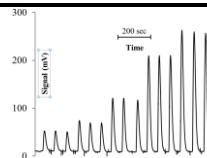
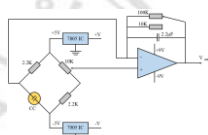
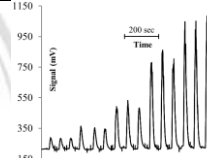
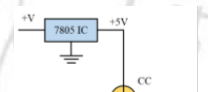
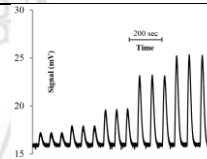
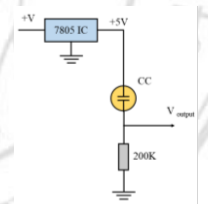
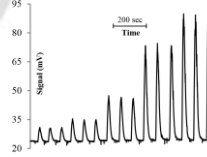
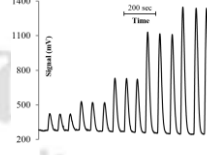
Figure 3.2 Wheatstone bridge circuit

$$V_{\text{output}} = V_{\text{input}} \left(\frac{R_{\text{cell}}}{R_2 + R_{\text{cell}}} - \frac{R_3}{R_3 + R_1} \right) \quad [3.2]$$

All DC conductivity detectors were placed in identical single-FI condition setup as explained in experimental section. DI water was used as the carrier stream with 1.0 mL min⁻¹ solution flow rate. The KCl standard solution series of 10-100 μmol L⁻¹ was injected into the flow system. Both formats of DC conductivity circuit were compared with the commercial pulse conductivity detector (712 conductometer, Metrohm) as shown the result in Table 3.1. The results show the linear relationship equation, standard deviation of baseline (SD_b) and the ratio of a peak height/standard deviation of baseline (PS/SD_b) of various format of conductivity detectors. All DC conductivity detectors provided the linear relationship with KCl concentration. The commercial conductometer (Methohm) provided the best slope of equation (sensitivity) but the SD_b was higher than the other detectors. The detector with 7805/7815-IC based format provided a well-defined FI-gram and lowest SD_b but the sensitivity was not high. Meanwhile, the ±9V-WB-OA format provided the best PS/SD_b ratio, unfortunately the FI-gram of ±9V-WB-OA was not a well-defined peak. This would come from the higher rate of gas bubble evolution at the electrode and make the fluctuation of measuring signal. However, the ±5V-WB-OA

provides a well-defined peak and good sensitivity as illustrated in Figure 3.3. Therefore, the $\pm 5V$ -WB-OA was selected to use as the DC conductivity detector for the next experiment for gas diffusion flow injection system and DIC determination.

Table 3.1 Comparison of the fabricated DC conductivity detectors performance

DC conductivity Detector	Linear equation	SD _b * (mV)	PS/ SD _b ratio**	Circuitry diagram format	FI-gram
$\pm 5V$ -WB-OA	$Y=2.31X + 16.8,$ $r^2=0.999$	0.5	83.3 ± 2.2		
$\pm 9V$ -WB-OA	$Y=8.39X + 29.9,$ $r^2=0.991$	0.7	98.0 ± 4.2		
7805 IC	$Y=0.09X + 0.28,$ $r^2=0.998$	0.1	12.3 ± 0.1		
7815 IC	$Y=0.65X + 1.26,$ $r^2=0.996$	0.2	38.3 ± 0.9		
Metrohm 712**	$Y=10.1X + 42.1,$ $r^2=0.999$	2.8	50.9 ± 0.8		

*SD_b is standard deviation of baseline signal of > 200 data points.

** The ratio of peak height signal of $10 \mu\text{mol L}^{-1}$ KCl and SD of baseline signal (average \pm SD). The SD = standard deviation which was calculated from 3 replicated of $10 \mu\text{mol L}^{-1}$ KCl injections.

*** The commercial pulse detector establishes analog out signal (0-2V) and acquired to computer through external DAQ. The device allows user to change the cell constant and as a result the analog signal can be amplified.

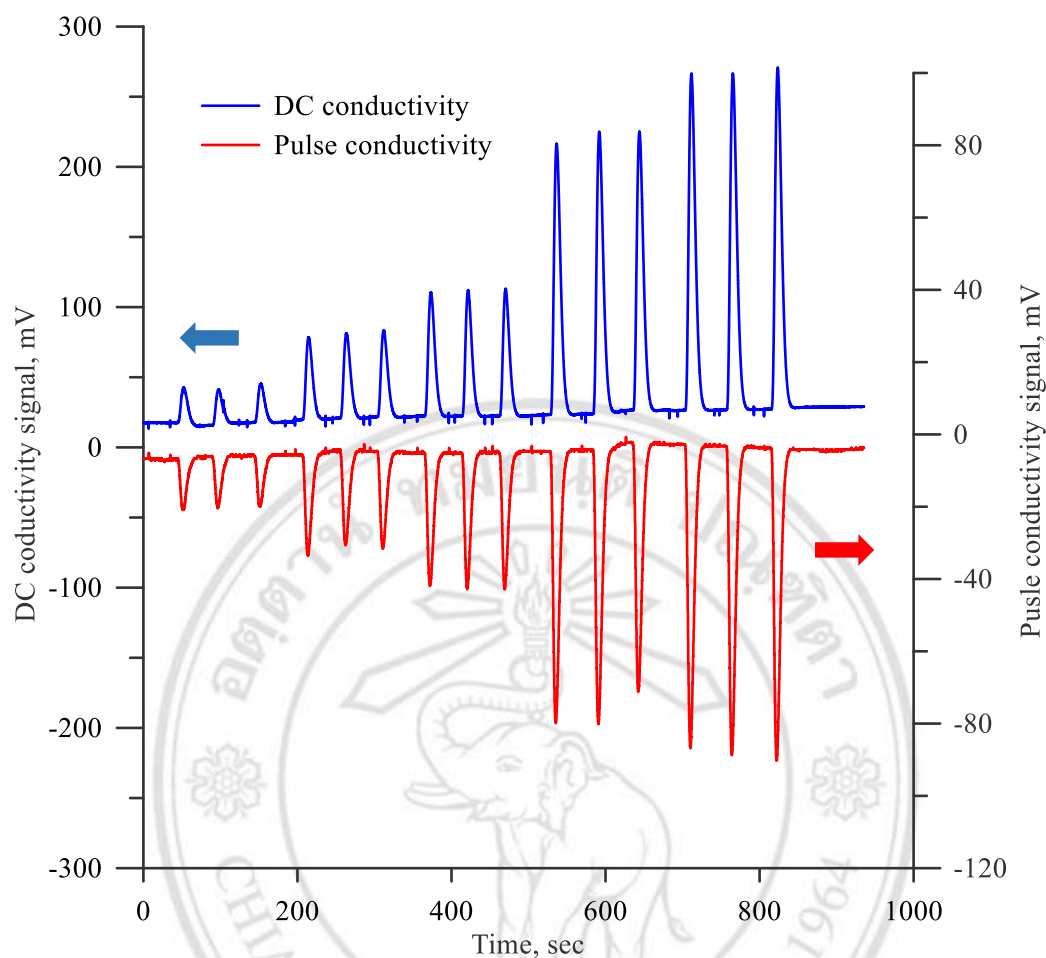


Figure 3.3 Comparison of FI-gram signal of 10-100 $\mu\text{mol L}^{-1}$ KCl injection in a single-FI of investigating DC-conductivity detector, blue line ($\pm 5\text{V-WB-OA}$) and a commercial pulse conductivity detector (712 Metrohm) which the signal is shown in inverse signal, red line

The reproducibility of $\pm 5\text{V-WB-OA}$ was also investigated. The experimental condition was setup as a single-FI. DI water was used as a carrier stream with 1.0 ml min^{-1} solution flow rate. The $60 \mu\text{mol L}^{-1}$ of KCl standard solution was injected into the flow system with 40 injections continuously as shown in Figure 3.4. As a result, the relative standard deviation (%RSD) of peak height was obtained approximately 3%. In some experiment, the $\pm 5\text{V-WB-OA}$ was supplied the voltage from two 9V-battery to replace the desktop power supply ($\pm 12\text{V DC}$) and was expected for portable setup in the future. The $100 \mu\text{mol L}^{-1}$ of KCl standard solution was injected into the DI water as a carrier stream with 1.0 mL min^{-1} flow rate hourly (8 hours) as illustrated in inset of Figure

3.4. The relative standard deviation (%RSD) of peak height signal was ~4.5%. This detector could be available to develop in future for the field measurement.

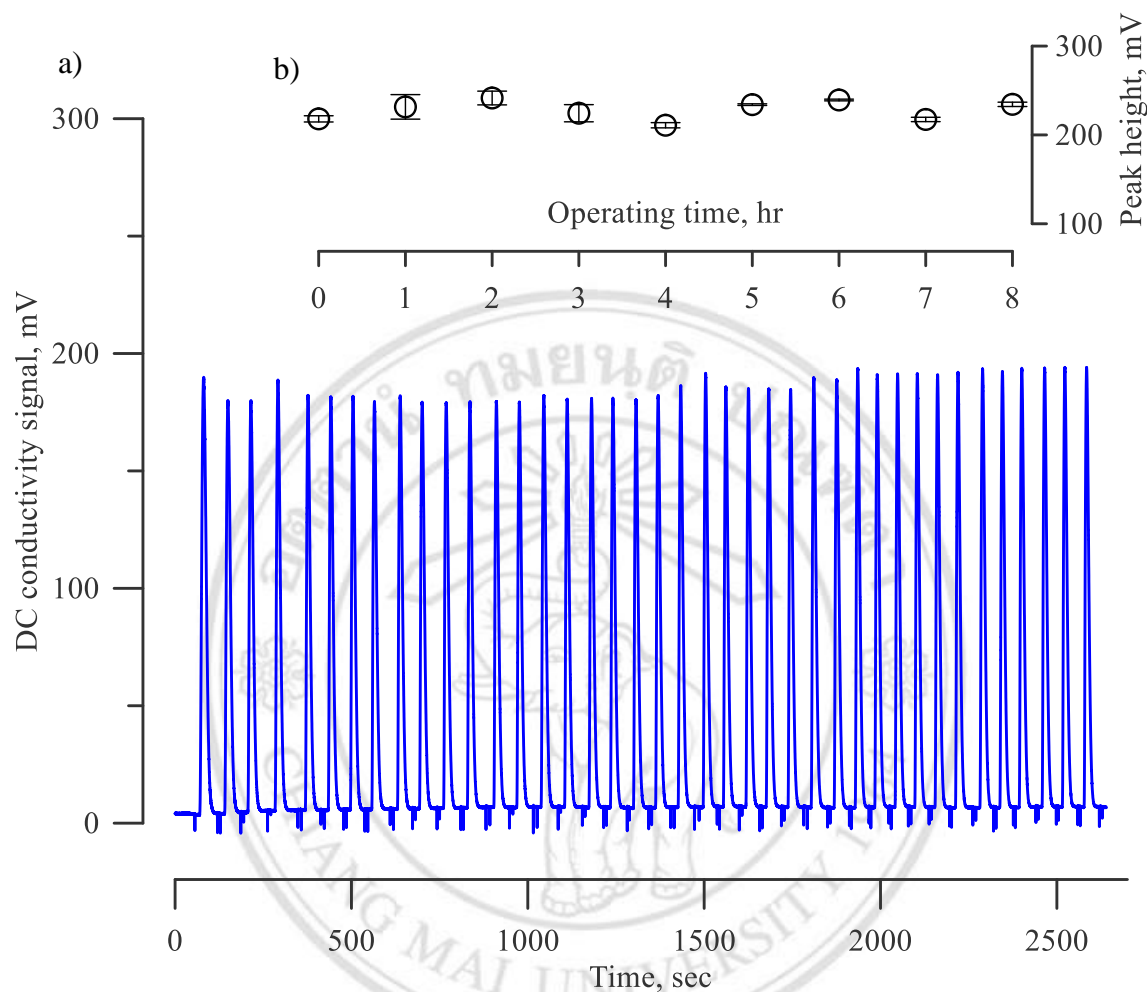


Figure 3.4 The FI-gram of standard KCl injections for investigation the repeatability of DC- conductivity detector: a) The 40 injections of $60 \mu\text{mol L}^{-1}$ KCl in 1.0 mL min^{-1} of water stream solution with using the external power from $\pm 12\text{V}$ desktop power supply and b) The signal of DC-conductivity detector along 8 hours using two 9V-battery

The applied potential and flow rate of carrier solution were also investigated as shown the result in Figure 3.5. Since, the carrier flow rate affects to the mass transfer and the removal gas bubble on the surface of electrodes/cell. In the experiment, the 1, 10 and $100 \mu\text{mol L}^{-1}$ KCl standard solutions were injected into the DI water as a carrier stream with various flow rates ($0.1\text{-}1.5 \text{ mL min}^{-1}$) in a single-FI system. From the result shown in Figure 3.5, 0.1 mL min^{-1} flow rate provided the highest peak height but FI-gram was not a well-defined peak and the SD of peak height signal was also higher. While the

increasing of carrier flow rate provided the lower peak height signal since the higher flow rate provides the less of ionic mass transfer to the electrode. Moreover, the higher flow rate provides the lower standard deviation of baseline since gas bubble was removed from electrode efficiently and as a result provide lower fluctuation of the measuring signal. This result agreed with those with using DC conductivity detector for ion chromatography (IC) by Qi et al [54]. The carrier flow rate was also described.

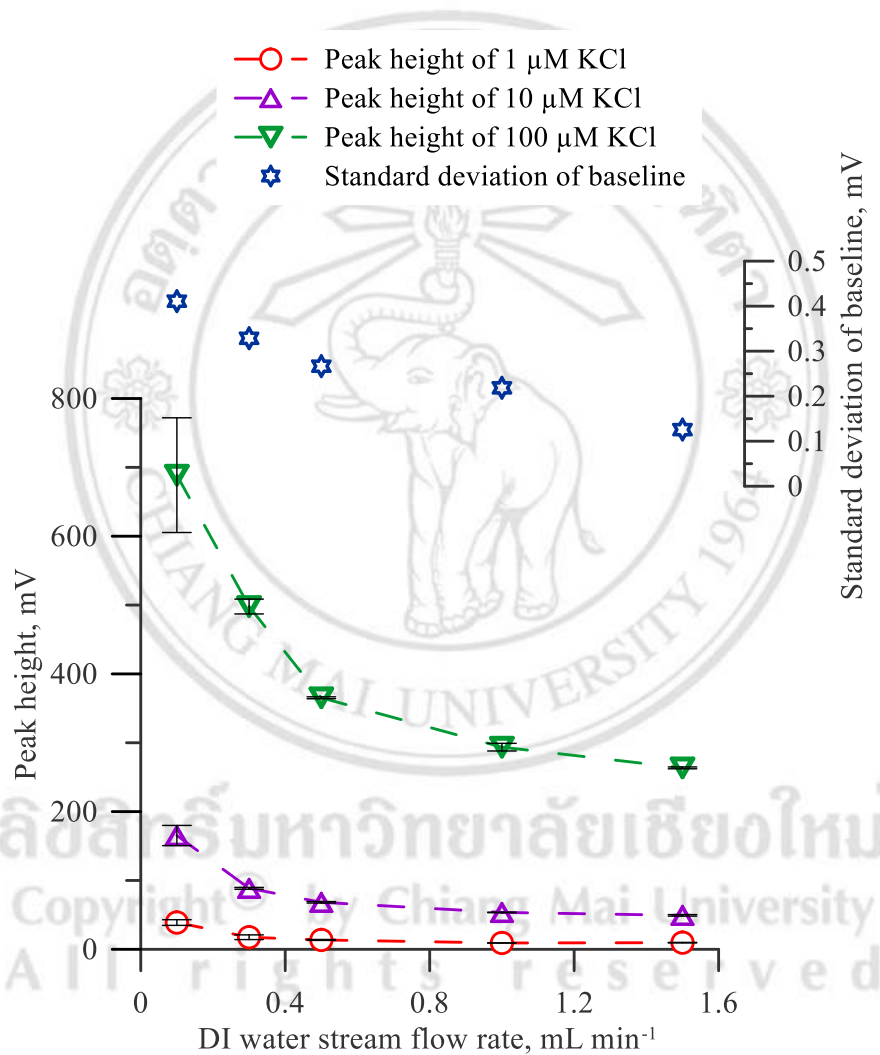


Figure 3.5 The peak height signal of KCl and standard deviation of baseline signal with various stream flow rate of carrier in single line FI system

Moreover, the digital multimeter (Unit-T 60A) was investigated to be used as a simple DC conductivity detector. The ohmmeter mode of multimeter is functioned based on the applying DC potential to the probes and measuring the returned current due to the

conductance of substrate. Then, the resistance is converted to conductance from the returned current. The resistance signal was recorded through the built-in RS232-PC interface and the conductance value was acquired to computer through their vendor program. The peak signal was also compatible to open and further analysis with Microsoft Excel program. In this experiment, the multimeter was connected to the conductivity flow cell as DC detector and operating in ohmmeter mode. The KCl standard solution of 10-100 $\mu\text{mol L}^{-1}$ was injected into the DI water as a carrier stream with 1.0 mL min^{-1} flow rate. As a result, the peak height was obtained and proportion to the concentration of KCl solutions. Nevertheless, its sensitivity is not high as the fabricated DC detector, it would be interesting simple tool for some other chemical analysis systems.

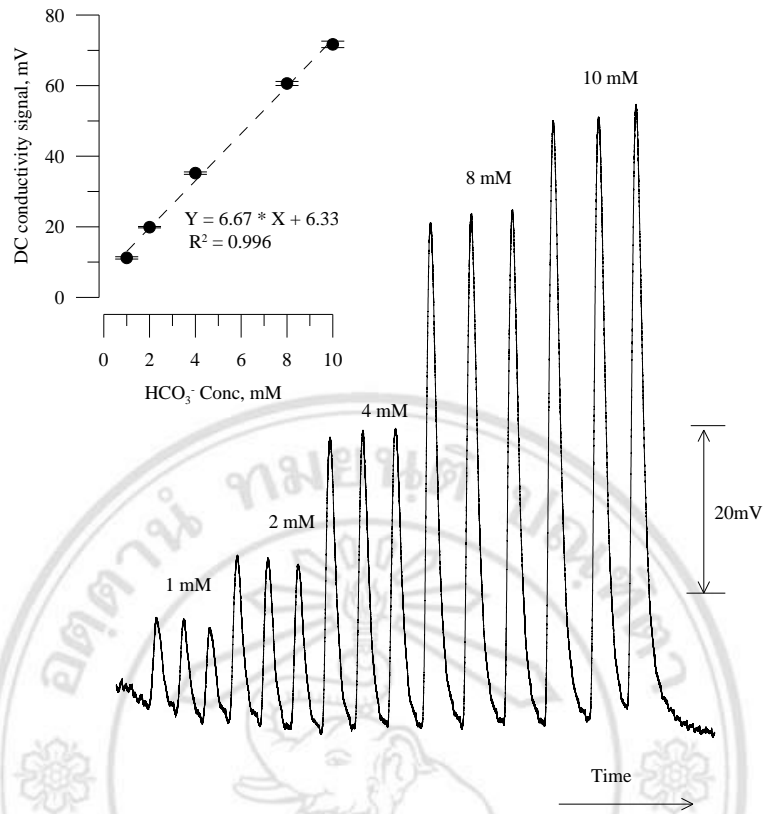
3.1.2 DC-conductivity detector coupled with GD-FI system

In the previous section study, the $\pm 5\text{V}$ -WB-OA based DC conductivity detector was selected to be used in this study because it provided the higher peak height signal, a good PS/SD_b ratio and a well-defined peak. In this experimental section, the detector was used with the GD-FI system. The GDU was used in the FI system for improving the selectivity of chemical analysis. The GDU comprises of double line solution stream as illustrated in Figure 2.8. Both solution lines are separated by using the Teflon tape membrane as the hydrophobic gas membrane. The only hydrophobic gas molecules can permit through the Teflon tape. The GD-FI approach is based on the injection of a gas convertible ion as HCO_3^- , CO_3^{2-} , NH_4^+ , SO_3^{2-} , S^{2-} into a continuous donor solution stream. The ions zone is reacted with the appropriate condition of donor stream to produce the analyte gas. The gas (CO_2 , NH_3 , SO_2 , H_2S) would be allowed to pass through the hydrophobic porous membrane to dissolve in an acceptor solution stream. The dissolved ion was detected with the DC conductivity detector. All analytical results of this section was obtained without the optimized condition of the flow system.

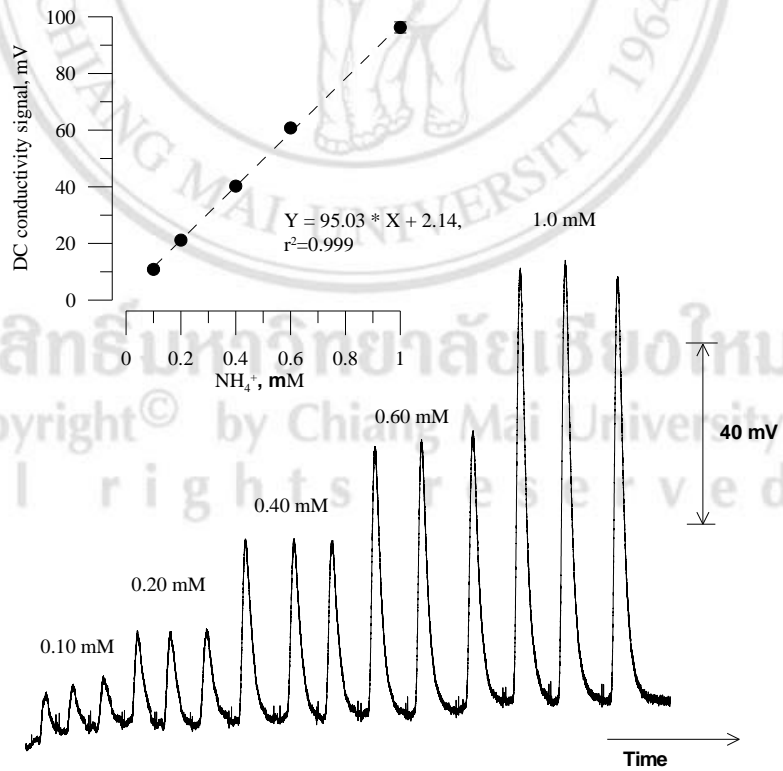
The 1.0-10 mmol L^{-1} of sodium bicarbonate standard solution was injected into the GD-FI system. The 0.1 mol L^{-1} phosphoric acid was reported as the lowest volatile acid solution and suitable for a donor solution stream [55]. DI water was used as an acceptor solution stream. Both solution stream flow rate was set as 1.0 mL min^{-1} . As a result, the signal of HCO_3^- could be detected with the DC conductivity detector. The GD-FI gram and the calibration graph were shown in Figure 3.6a. Not only the good linearity

of a calibration graph could be obtained as Peak height, (mV) = 6.67[HCO₃⁻], (mmol L⁻¹) + 6.33, r² = 0.996 but also the GD-FI gram was a well-defined peak. The 1.0-10 mmol L⁻¹ of sodium sulfide standard solution was also injected into the GD-FI based with DC detector as the identical flow condition. The GD-FI gram using DC conductivity detector was compared with the commercial pulse conductometer (712 Metrohm) as illustrated in Figure 3.6c. The two of identical conductivity flow cells were fabricated and arranged in series in GD-FI system for comparison the signal of the proposed detector with a commercial pulse conductivity detector as shown in Figure 3.11. As a result, the GD-FI gram of proposed detector was a well-defined peak and the calibration graph could be obtained as Peak height, (mV) = 3.92[S²⁻], (mmol L⁻¹) + 5.76, r² = 0.986. Moreover, the 0.1-1.0 mmol L⁻¹ of ammonium chloride standard solution was injected into the GD-FI system. The 0.1 mol L⁻¹ NaOH solution was used as a donor solution stream replacing the H₃PO₄ solution. Ammonium ion could be converted to NH₃ gas in a basic solution. The DI water was used as an acceptor solution stream and the flow rate of both solution stream was set as 1.0 mL min⁻¹. A well-defined peak in GD-FI gram was obtained as illustrated in Figure 3.6b. The linearity relationship of calibration graph was obtained as Peak height, (mV) = 95.03 [NH₄⁺], (mmol L⁻¹) + 2.14, r² = 0.999. Therefore, the proposed DC detector can be used with the GD-FI system for HCO₃⁻, S²⁻ and NH₄⁺ detection.

a)



b)



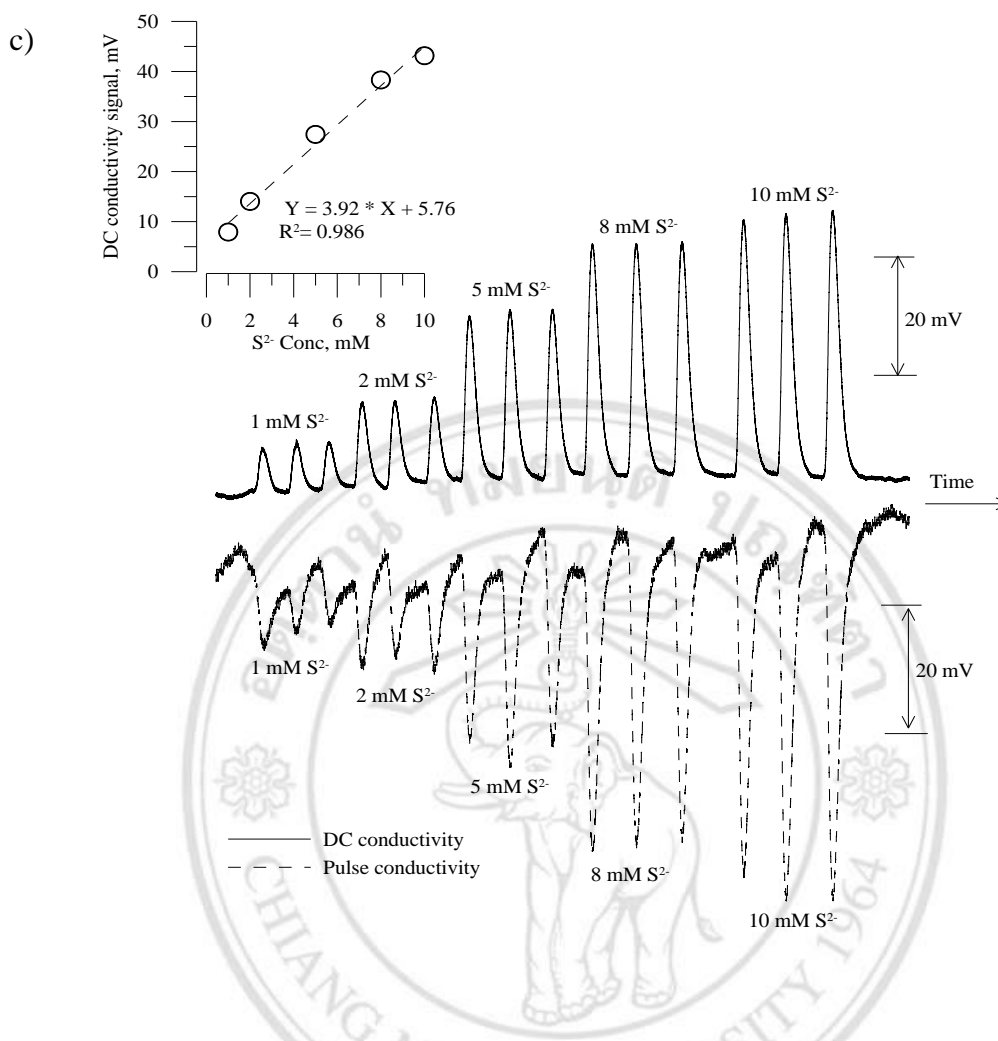


Figure 3.6 Typical GD-FI gram and calibration graph with DC conductivity detector. a) 1.0-10 mmol L⁻¹ HCO₃⁻ b) 0.1-1.0 mmol L⁻¹ NH₄⁺ c) 1-10 mmol L⁻¹ S²⁻; comparison with pulse conductometer which the signal is shown in inverse signal, dash line (40 μL injection volume with 20 cm length-mixing coil, 1.0 mL min⁻¹ flow rate of both carrier, DI water as acceptor solution stream and 0.1 mol L⁻¹ H₃PO₄ as a donor solution stream for HCO₃⁻, S²⁻ detection and 0.1 mol L⁻¹ NaOH as a donor stream for NH₄⁺ detection)

3.1.3 Optimization of GD-FI system for DIC determination

The dissolved inorganic carbon (DIC) was selected to be an application of the proposed DC conductivity detector coupled with the GD-FI system since the typical amount of DIC in the natural water is in the range of 1.0-10 mmol L⁻¹ [6], which appropriates with the detection ability of the proposed method. Some analytical parameters such as typical acid solution, concentration of acidic donor solution, flow rate

of donor and acceptor solution were studied to get more understand the limitation of this DC conductivity detector coupled with GD-FI system.

The DC conductivity detector was successfully used with the DI water stream as an acceptor solution since DI water provided the lower standard deviation of baseline (SD_b) and a well-defined peak. The lower concentration of NaOH solution has also reported as an acceptor stream to improve HCO_3^- trapping efficiency and as a result to enhance the limit of detection for DIC determination [6]. The 10 and 25 $\mu\text{mol L}^{-1}$ NaOH solution were investigated to this concept as an acceptor solution stream in GD-FI system. The NaOH solution was replaced DI-water in an acceptor solution stream and 10 mmol L^{-1} HCO_3^- was injected into GD-FI system, the GD-FI grams were compared as illustrated in Figure 3.7a. The higher concentration of NaOH solution provided a lower peak height signal of HCO_3^- , higher standard deviation of baseline and poor peak shape. Because the higher conductivity of NaOH solution promoted more the electrolytic reaction of water and produced more gas bubble. The higher flow rate of acceptor stream might be required to remove the gas bubble efficiently but the peak height signal of HCO_3^- might be also low because of the lower dissolving of analyte gas in an acceptor stream. In addition, the boiled DI water was suggested to use as an acceptor solution stream in GD-FI system for the HCO_3^- detection. The boiled DI water was expected to eliminate the dissolved CO_2 species in the acceptor stream. Both types of water were investigated to use as an acceptor stream and compared the GD-FI gram of injected 10 mmol L^{-1} HCO_3^- as illustrated in Figure 3.7a with blue lines. Both types of water provided similar peak height signals significantly. In addition, the tap water has also been used as an acceptor stream in GD-FI system. But the fluctuating signal of baseline was appeared since the tap water contains many ions especially dissolved chloride ion. Therefore, the DI water was selected to use as an acceptor stream in GD-FI system for DIC detection.

The flow rate of an acceptor solution stream was investigated. The 5 mmol L^{-1} HCO_3^- was injected into the 0.1 mol L^{-1} H_3PO_4 as a donor solution stream with a constant flow rate of 1.0 mL min^{-1} . The flow rate of 0.5-3.2 mL min^{-1} was set for DI water as an acceptor stream. The 1.0 mL min^{-1} flow rate provided the highest peak height signal and will be selected to use as the acceptor flow rate for DIC detection. The higher flow rates of an acceptor stream provided the lower standard deviation of baseline signals to correlate the previous result.

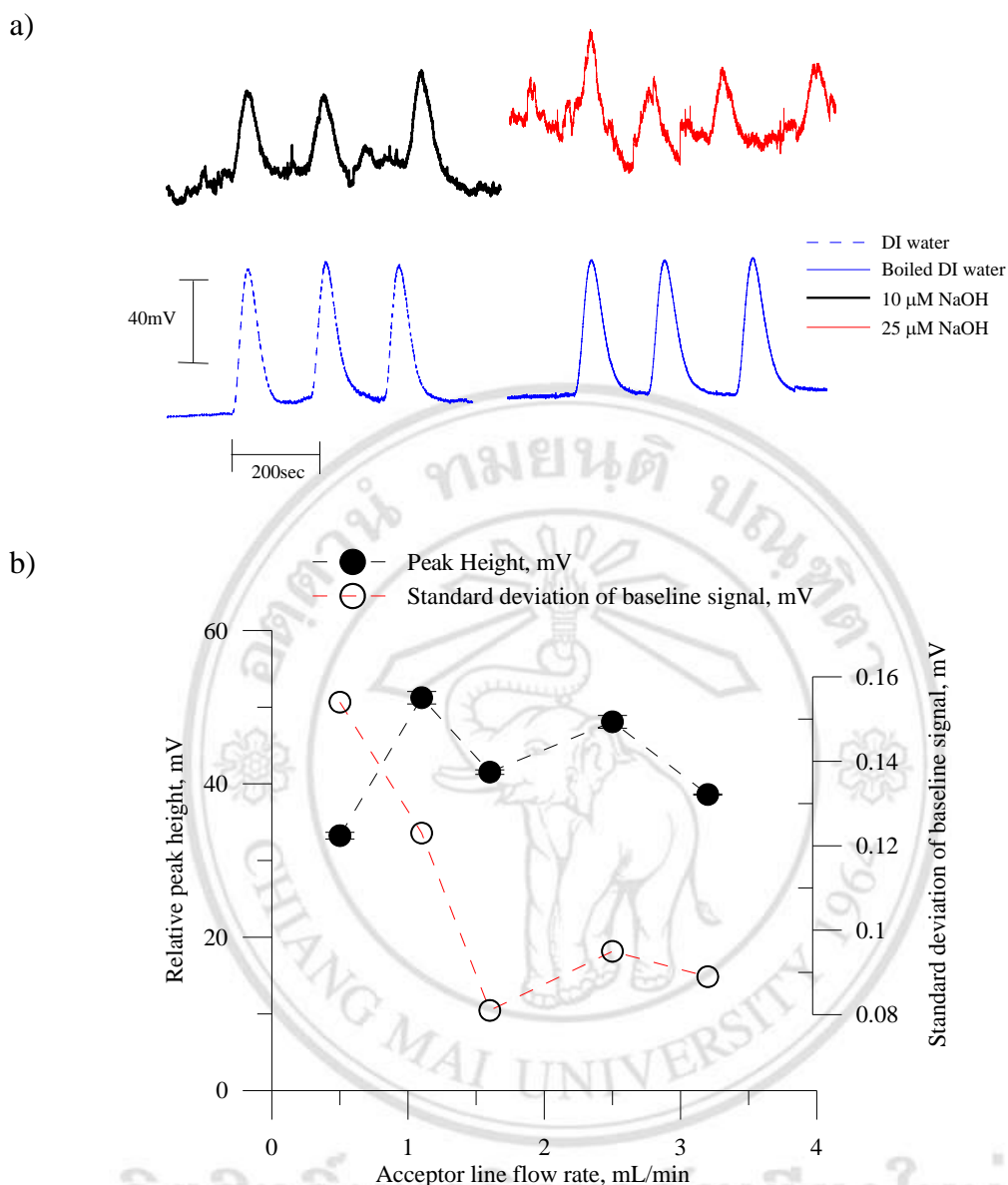


Figure 3.7 Optimization of an acceptor stream in GD-FI system using DC conductivity detector for DIC determination with using 1.0 mL min^{-1} of $0.1 \text{ mol L}^{-1} \text{ H}_3\text{PO}_4$ as a donor stream: a) Signal of $10 \text{ m mol L}^{-1} \text{ HCO}_3^-$ in 1.0 mL min^{-1} of various solution types of acceptor stream, b) Signal of $5 \text{ mmol L}^{-1} \text{ HCO}_3^-$ in various flow rates of DI-water acceptor stream ($0.1 \text{ mol L}^{-1} \text{ H}_3\text{PO}_4$ with flow rate of 1.0 mL min^{-1} as a donor stream)

Moreover, the parameters of donor solution stream such as the concentration of acid solution and the flow rate of a donor stream, affects to the analytical performance for DIC determination. Firstly, the concentration of acid solution was investigated. The phosphoric acid solution was selected as a donor solution stream. The $0.001\text{-}0.1 \text{ mol L}^{-1} \text{ H}_3\text{PO}_4$ was used as a donor stream with a constant flow rate of 1.0 mL min^{-1} and DI water

was used as an acceptor stream. The $10 \text{ mmol L}^{-1} \text{HCO}_3^-$ was injected in GD-FI system to evaluate the obtained peak height signal as illustrated in Figure 3.8a. The $0.01 \text{ mol L}^{-1} \text{H}_3\text{PO}_4$ was selected because the peak height signal was not significantly different with $0.1 \text{ mol L}^{-1} \text{H}_3\text{PO}_4$ and enough to produce the analyte gas. The sulfuric acid solution was also used as a donor solution with the same experimental condition. The result was similar to phosphoric acid solution. For second parameter, the flow rate of donor solution stream was set as 0.5 , 1.0 and 1.5 mL min^{-1} by using $0.1 \text{ mol L}^{-1} \text{H}_3\text{PO}_4$ as a donor solution and the acceptor stream was set as same as the previous experiment. The $5 \text{ mmol L}^{-1} \text{HCO}_3^-$ was injected in GD-FI system. As a result, the 0.5 mL min^{-1} flow rate provided the highest peak height signal and was selected to use as the donor flow rate. Because the slower flow rate of a donor stream provided a longer time of HCO_3^- zone merged with the donor solution, thus the analyte gas was more produced. These optimized conditions were applied to use in the GD-FI system coupled with the DC detector for DIC determination in the natural water and the analytical performance of the proposed method was reported in the next section.



ลิขสิทธิ์มหาวิทยาลัยเชียงใหม่
Copyright© by Chiang Mai University
All rights reserved

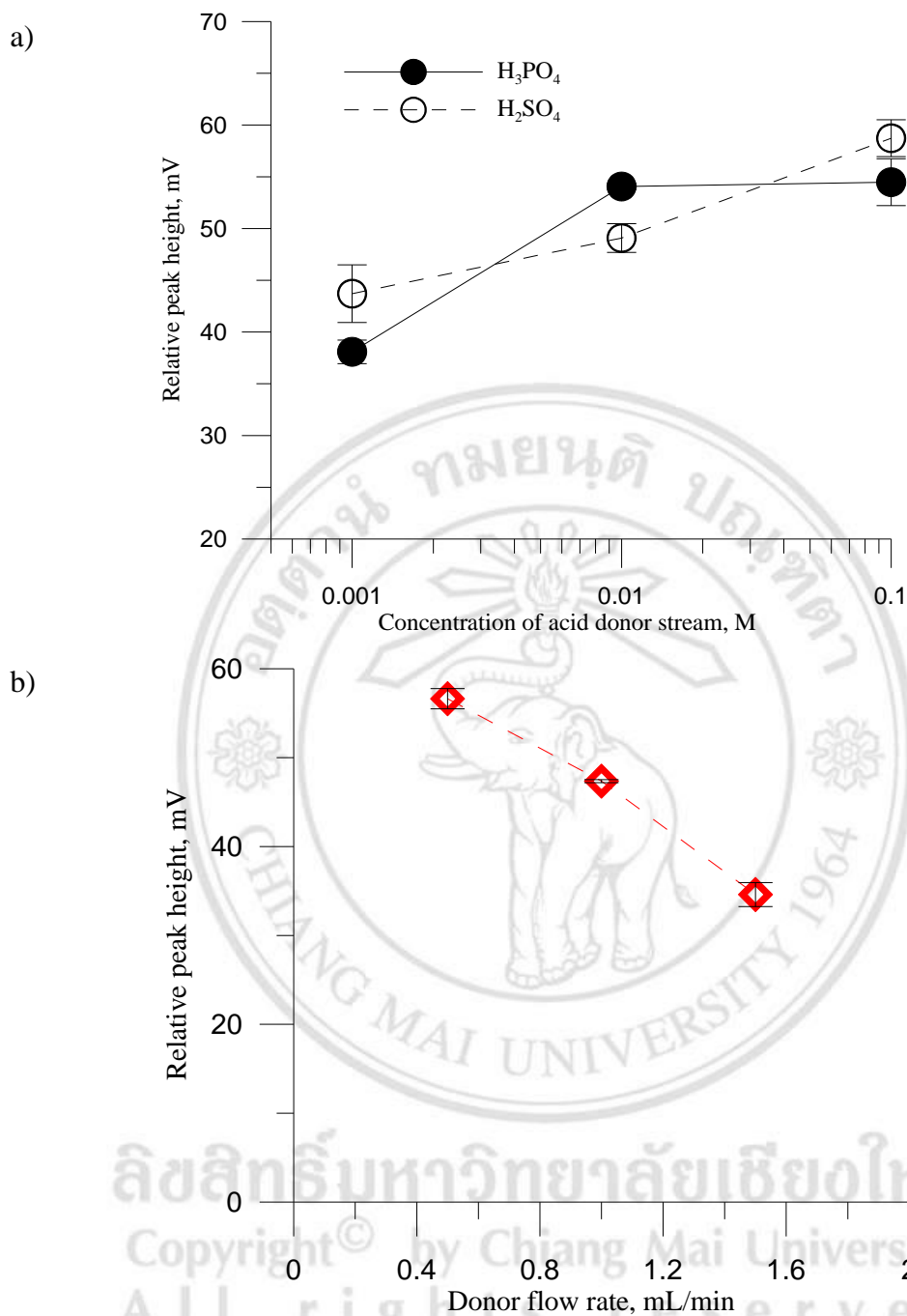


Figure 3.8 Optimization of an acidic donor solution in GD-FI system using DC conductivity detector for DIC determination with using 1.0 mL min^{-1} of DI water as an acceptor stream: a) Injection of $10 \text{ mmol L}^{-1} \text{ HCO}_3^-$ in various acid concentrations and typical acid solution and b) Injection of $5 \text{ mmol L}^{-1} \text{ HCO}_3^-$ in various flow rates of $0.1 \text{ mol L}^{-1} \text{ H}_3\text{PO}_4$ as a donor stream

3.1.4 The analytical performance for DIC determination

In the optimized conditions, the $0.01 \text{ mol L}^{-1} \text{ H}_3\text{PO}_4$ was used as a donor solution with 0.5 mL min^{-1} flow rate and DI water was used as an acceptor solution with 1.0 mL min^{-1} flow rate. As a result, the linear working range of DIC detection was obtained in the range of $1.0\text{-}10 \text{ mmol L}^{-1} \text{ HCO}_3^-$ with sample throughput of $15 \text{ injections h}^{-1}$. The $6 \text{ mmol L}^{-1} \text{ HCO}_3^-$ was injected in the GD-FI system with 7 injections. The relative standard deviation (%RSD) of $<3\%$ was obtained as demonstrated in Figure 3.9. The limit of detection (LOD) based on 3 times of a standard deviation of blank was $70 \text{ }\mu\text{mol L}^{-1} \text{ HCO}_3^-$. The proposed DC conductivity detector might be used for determination of the other gas convertible species such an ammonium ion.

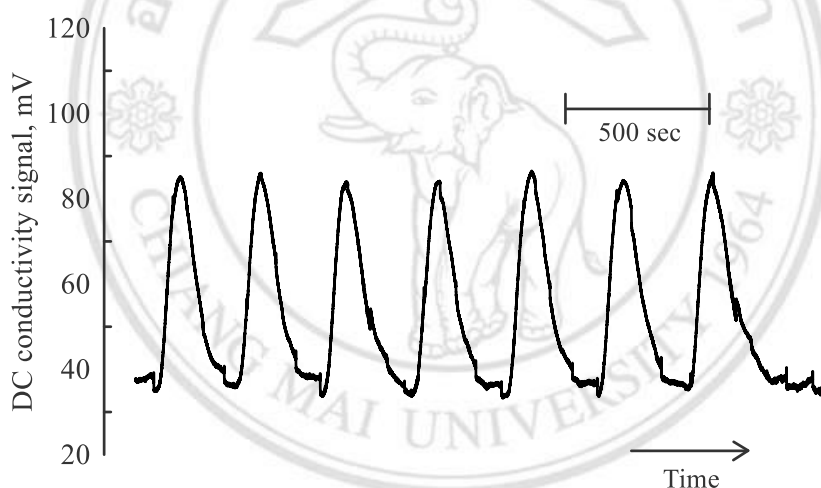
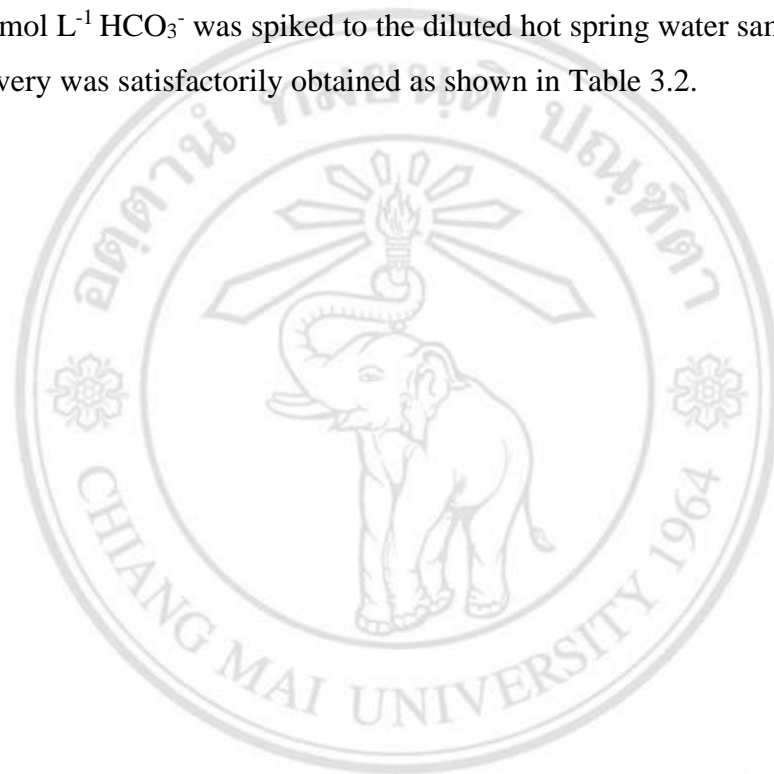


Figure 3.9 The GD-FI gram of 7 injections of $6 \text{ mmol L}^{-1} \text{ HCO}_3^-$ ($40 \text{ }\mu\text{L}$ injection volume with 20 cm length-mixing coil, 1.0 mL min^{-1} flow rate of both carrier, DI water as acceptor line and $0.1 \text{ mol L}^{-1} \text{ H}_3\text{PO}_4$ as donor line)

The proposed method was applied for DIC determination in hot spring water samples. The sulfide (S^{2-}) and sulfite (SO_3^{2-}) ion are considered as major interference in the hot spring water sample. In the acidic solution, both sulfide/ sulfite interferences can be converted to H_2S and SO_2 gas, respectively. As a result, the DC conductivity based GD-FI system can be interfered from those ions. The addition of KMnO_4 , Cr(IV) and H_2O_2 were suggested to eliminate the sulfide and sulfite ion [29]. The KMnO_4 was

selected for investigating the removal of sulfide and sulfite ion because KMnO_4 is a strong oxidizing agent which can oxidize S^{2-} and SO_3^{2-} ion to be SO_4^{2-} ion, which can not convert to gaseous species. In the experiment, $2 \text{ mmol L}^{-1} \text{HCO}_3^-$ was mixed with the $1\text{-}2 \text{ mmol L}^{-1}$ of S^{2-} and SO_3^{2-} and $5 \text{ mmol L}^{-1} \text{KMnO}_4$ as illustrated in Figure 3.10. The $5 \text{ mmol L}^{-1} \text{KMnO}_4$ was successful to eliminate the major interference in the hot spring water. The KMnO_4 solution was added to the hot spring water sample in the sample preparation procedure. In addition, the accurate result was expressed with recovery percentage. The 1.0 and $3.0 \text{ mmol L}^{-1} \text{HCO}_3^-$ was spiked to the diluted hot spring water samples. The 93-103% of recovery was satisfactorily obtained as shown in Table 3.2.



ลิขสิทธิ์มหาวิทยาลัยเชียงใหม่
Copyright© by Chiang Mai University
All rights reserved

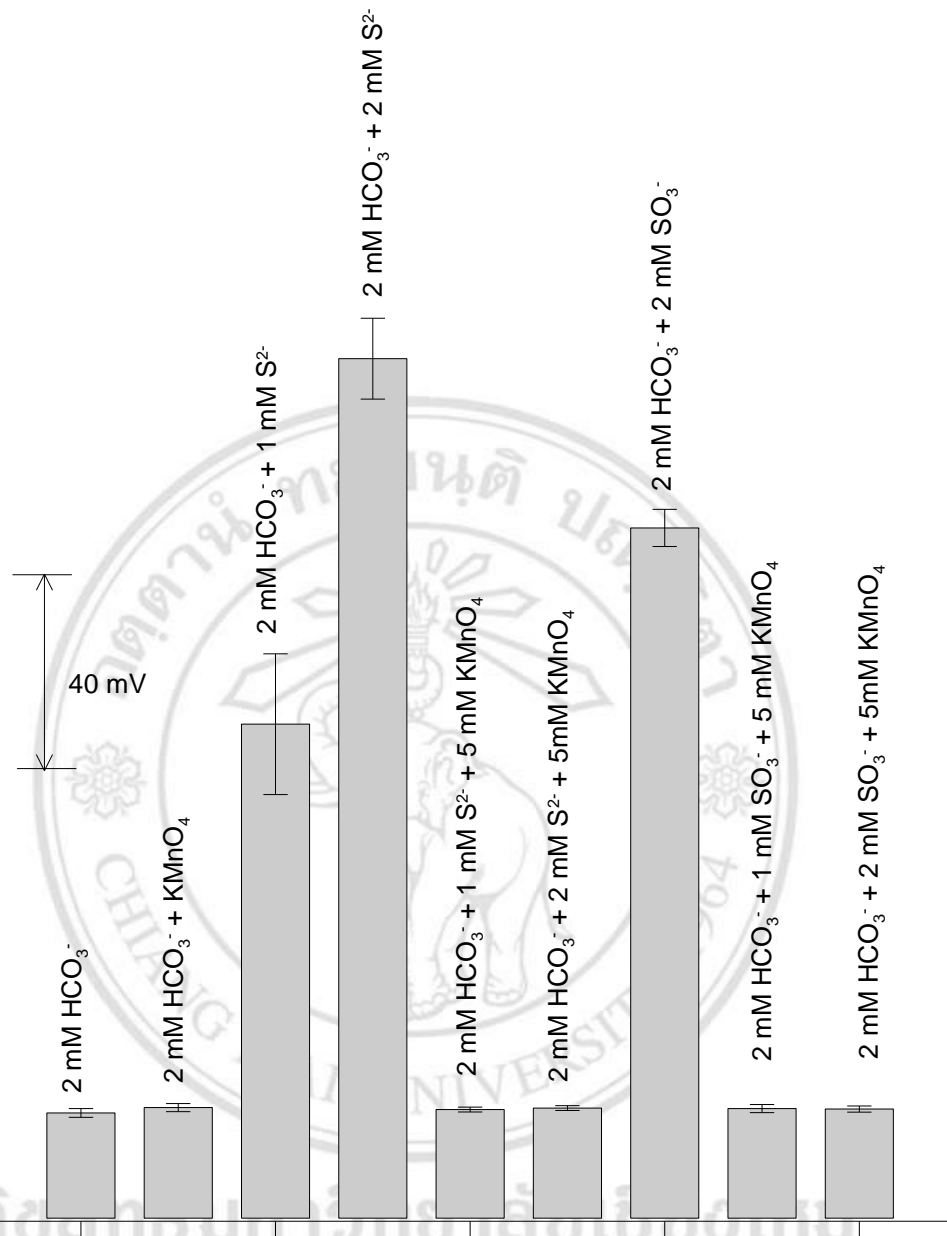


Figure 3.10 The comparison of signal of major interference studies for DIC determination and adding KMnO₄ for removing sulfide and sulfite ion as interference

Table 3.2 The recovery of DIC determination in hot spring water sample with proposed conductivity detector

Sample	HCO ₃ ⁻ added	DIC Found* (mM)	% Recovery
Hot spring water 1	0.0	4.18 ± 0.17	
	1.0	5.18 ± 0.14	100
	3.0	6.97 ± 0.08	93
Hot spring water 2	0.0	4.32 ± 0.00	
	1.0	5.34 ± 0.11	102
	3.0	7.32 ± 0.05	100
Hot spring water 3	0.0	4.23 ± 0.03	
	1.0	5.24 ± 0.05	101
	3.0	7.04 ± 0.02	94
Hot spring water 4	0.0	4.26 ± 0.07	
	1.0	5.28 ± 0.05	102
	3.0	7.28 ± 0.11	101
Mineral water	0.0	2.37 ± 0.06	
	1.0	3.40 ± 0.10	103
	3.0	5.44 ± 0.05	102

*The value is average ± SD (3 replicates)

Many detection methods were used with the GD-FI system for DIC determination in water sample. The analytical performance of the proposed DC conductivity detector was compared with the other detection methods, for example the linear range of calibration graph, the limit of detection (LOD), the relative standard deviation (%RSD), and sample throughput as demonstrated in Table 3.3. The fabricated DC conductivity detector is an extremely low cost detection unit with approximate cost about 120\$ USD (including DAQ unit). Also, it can be fabricated easily without the part of a frequency generator and pulse rectifier circuits. In addition, the proposed detector can be used with a 9V-battery (Model Energizer Max) replacing the desktop power supply and the battery voltage was monitored throughout operating time for 8 h. The battery voltage decreases in the range of 9.6 to 8.8 V with a good reproducibility signal as previous discussion. The detector shows the low consumption energy. The detector has been progressing to be a portable unit for on-site measurement.

Table 3.3 Performance of the GD-FI system with the proposed DC conductivity detector for DIC determination comparing with other previous methods

Detectors	Analytical applications	Linear range (mM)	LOD (μM)	%RSD	Sampling rate (h^{-1})	Ref.
Potentiometry	Water	0.08-1.7	3	1.4	30	[27]
Potentiometry	Vines	1-11		2	50	[33]
Pulse conductivity	Natural water	0.05-5.00	10	3.4		[6]
Pulse conductivity	Lake Water	0.05-0.5	3	1.2	45	[7]
Pulse conductivity	Natural water	1.75-5.00	3	4.8-9	15	[29]
Pulse conductivity	Seawater	2.0-9.0	50	< 1	15	[5]
CCD**	Water	0.01-1	6	4.1	15	[30]
CCD**	Estuarine water	0.2-10	80	0.32	90	[26]
Capacitance sensor	Water		0.8	2.3		[56]
Spectrophotometry	Natural water	up to 2.87	20		20	[25]
Spectrophotometry	Water	0.001-1	1	1.9	20	[24]
FTIR*	Water	up to 16	250	1.2-2.4	15	[31]
FTIR*	Natural water	up to 5	75	1.3	30	[32]
Chemiluminescence	Water	0.0001- 5	1.2×10^{-8}	5.1		[57]
Bulk acoustic wave	Natural/waste water	0.05-20.00	10	0.95	45	[28]
DC conductivity	Hot spring water	1.0-10	70	3	15	This work

* FTIR = Fourier transform infrared spectroscopy

**CCD = Contactless conductivity detector

3.1.5 Application of DIC determination in hot spring water sample

The DIC concentration in hot spring water and mineral drinking water samples were determined by using the proposed DC conductivity detector compared with the commercial pulse conductometer (712 Metrohm) in GD-FI system. Both detectors were set up in GD-FI system as series detectors by using two identical conductivity flow cells as shown in Figure 3.11b. The commercial pulse conductometer was placed in front of the proposed DC conductivity detector because of avoiding the produced ion from electrolytic reaction as illustrated in Figure 3.11a. The 8 samples of hot spring water and mineral drinking water were injected in the GD-FI system. The DIC concentration from both detectors were compared in Table 3.4. The paired *t*-test was used to investigate the proposed DC conductivity detector with the commercial pulse conductometer as a standard method. The calculated *t* value is less than the theoretical *t* value with a confidence interval of 95%. Hence, the proposed detector is not significantly different with the commercial pulse conductometer. The proposed detector can be an alternative detection method for DIC determination in GD-FI system.

Table 3.4 Comparison of DIC determination by using proposed detector and pulse conductivity detector

Sample	Dissolved inorganic carbon (mM)*	
	DC conductivity detector	Pulse conductivity detector
Hot spring water-1	7.26 ±0.30	6.94 ±0.20
Hot spring water-2	7.72 ±0.05	7.41 ±0.08
Hot spring water-3	7.76 ±0.15	7.35 ±0.18
Hot spring water-4	8.55 ±0.04	8.56 ±0.36
Hot spring water-5	9.21 ±0.20	9.24 ±0.19
Hot spring water-6	9.58 ±0.19	9.60 ±0.12
Mineral water-1	4.35 ±0.13	4.59 ±0.11
Mineral water-2	5.81 ±0.19	6.11 ±0.13

* The value is average ± SD of triplicate results.

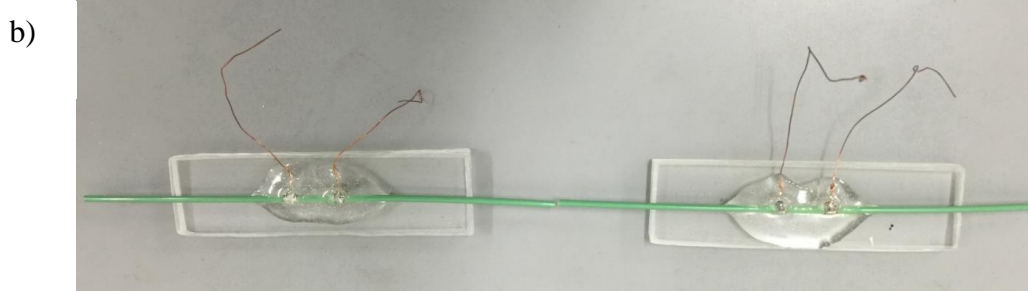
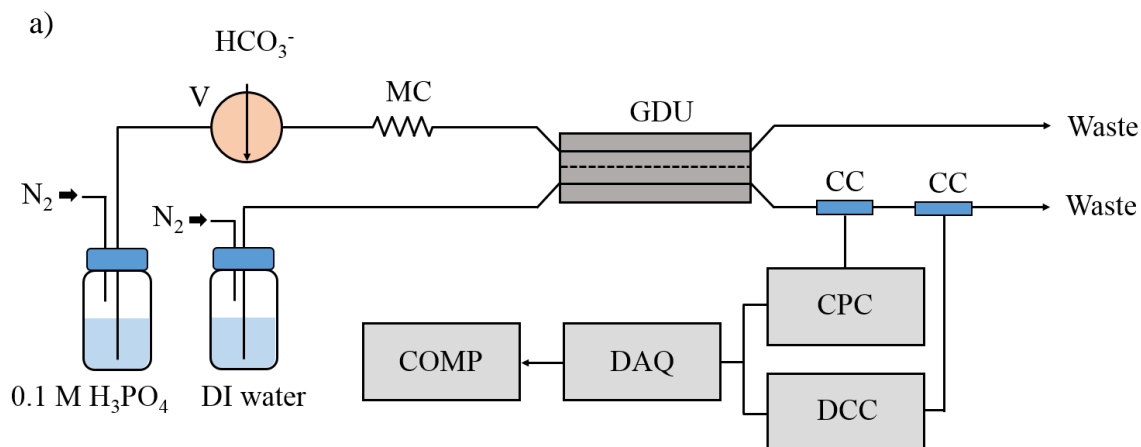


Figure 3.11 a) Schematic diagram of simple flow injection-gas diffusion unit with serial arrangement of pulse conductometer and DC-conductometer; V, 6-ports-2-positions injection valve; MC, mixing coil; GDU, gas diffusion unit; CC, conductivity cell; CPC, commercial pulse conductometer; DCC, direct current conductivity circuit; DAQ, data acquisition unit; COMP, computer and b) Photograph of two identical conductivity flow cells

ลิขสิทธิ์มหาวิทยาลัยเชียงใหม่
Copyright © by Chiang Mai University
All rights reserved

3.2 LED-photodiode based fluorescence detector with FI system for NH₄⁺ determination

The fluorescence based ammonium determination via the chemical reaction of OPA-sulfite [20], has been reported as highly sensitive and selectivity technique. This chemical solution containing ortho-Phthalaldehyde (OPA), sodium sulfite and phosphate buffer, was used as the carrier stream in single line FI system. The mixed OPA reagent of 10 mmol L⁻¹ OPA, 3 mmol L⁻¹ Na₂SO₃ and 0.1 mol L⁻¹ phosphate buffer pH 11.0 was suggested by Ohira et al. [17]. The 10 μmol L⁻¹ NH₄⁺ was merged with the OPA reagent in batch reaction and heated in 65°C water bath for 10 min. The fluorescence spectrum of NH₃-OPA-sulfite reaction product was measured. As a result, the maximum excitation and emission of the NH₃-OPA-sulfite product were obtained at 361 and 458 nm respectively as illustrated in Figure 3.12. The fluorescence spectra were obtained by using spectrofluorometer with the following setting: λ_{Ex} for Em: 362 nm, Ex slit: 5 nm, Em slit: 5 nm, scan speed: 60 nm min⁻¹, UV-LED: λ_{max} 365 nm, long-pass UV filter: sharp cut-on 400 nm. The UV-LED and UV filter spectra were modified from the official datasheet; NSHU591B, www.nichia.co.jp and UV Filter Sheet, www.edmundoptics.com, respectively.

The LED-photodiode based fluorescence detector used in this study was illustrated in Figure 2.5 and Figure 2.7. The appropriate light source and the long-pass optical filter were selected based on the fluorescence spectrum in Figure 3.12. The UV-LED was used to generate the 365 nm excitation light through the optical fiber to the cross junction area. The emitted fluorescence was detected by using integrated photodiode and built-in amplifier (OPT301) through an optical fiber and a long-pass optical filter sheet (400 nm shape cut-on) which disposed the scattered excitation light. The generated current from a photodiode was converted to voltage by built-in operational amplifier in OPT301 as following in Equation 3.3.

$$V_{\text{out}} = -I_{\text{in}} R_f \quad [3.3]$$

Where, V_{out} is output voltage, I_{in} is the generated current from photodiode and R_f is a feedback resistor as 1 MΩ. For 1 μA current, the obtained output voltage will be -1 V and then the output voltage was also amplified as 50 times by using FET-input operational amplifier (TL072) as following Equation 3.4.

$$V_{\text{output}} = - \left(\frac{R_f}{R_i} \right) V_{\text{in}} \quad [3.4]$$

Where, R_f is a feedback resistor, R_i is the resistor which connects to the inverting input of operational amplifier. As following Figure 2.5 (1/2 TL072 part), R_f and R_i is 1 M Ω and 20 K Ω , respectively. The amplifying ratio will be 50 times with inverted signal. In order to convert the amplified signal to a desired and appropriate polarity, the second operational amplifier is also added. Therefore, the output signal is proportional to the incident light intensity on a photodiode. In addition, the obtained fluorescence signal is depended on the intensity of excitation light which relates to the applied current of the light source. Hence, the UV-LED was applied the maximum current with 25 mA according to a limit of LED.

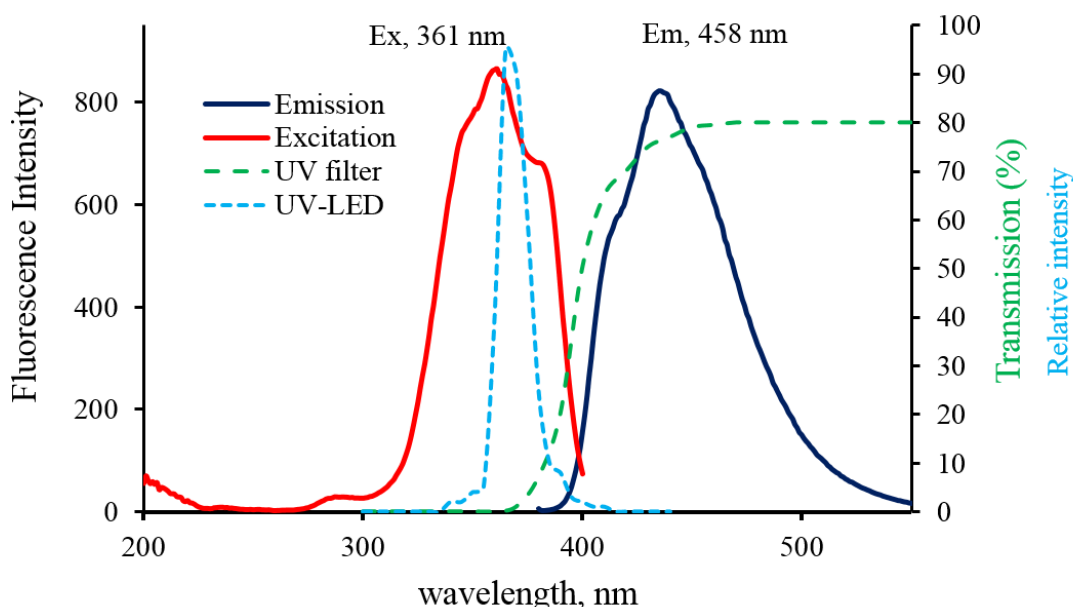


Figure 3.12 The fluorescence spectrum of chemical product of NH_3 -OPA-sulfite reaction in 0.1 mol L^{-1} phosphate buffer pH 11 and the overlaid spectra of UV-LED and UV filter

3.2.1 Some analytical characteristic in the FI system

The proposed fluorescence detector was applied in single line FI system. The fluorescence signal of the LED-photodiode based fluorescence detector was tested with standard fluorescein solution of 1.0-100 $\mu\text{mol L}^{-1}$. The fluorescein solution was injected into the DI water as a carrier stream with 1.2 mL min^{-1} flow rate. The FI-gram of fluorescein solution and the linear relationship of calibration graph were shown in Figure

3.13. As a result, the proposed fluorescenc detector was applicable to use with the fluorescence based ammonium-OPA-sulfite reaction.

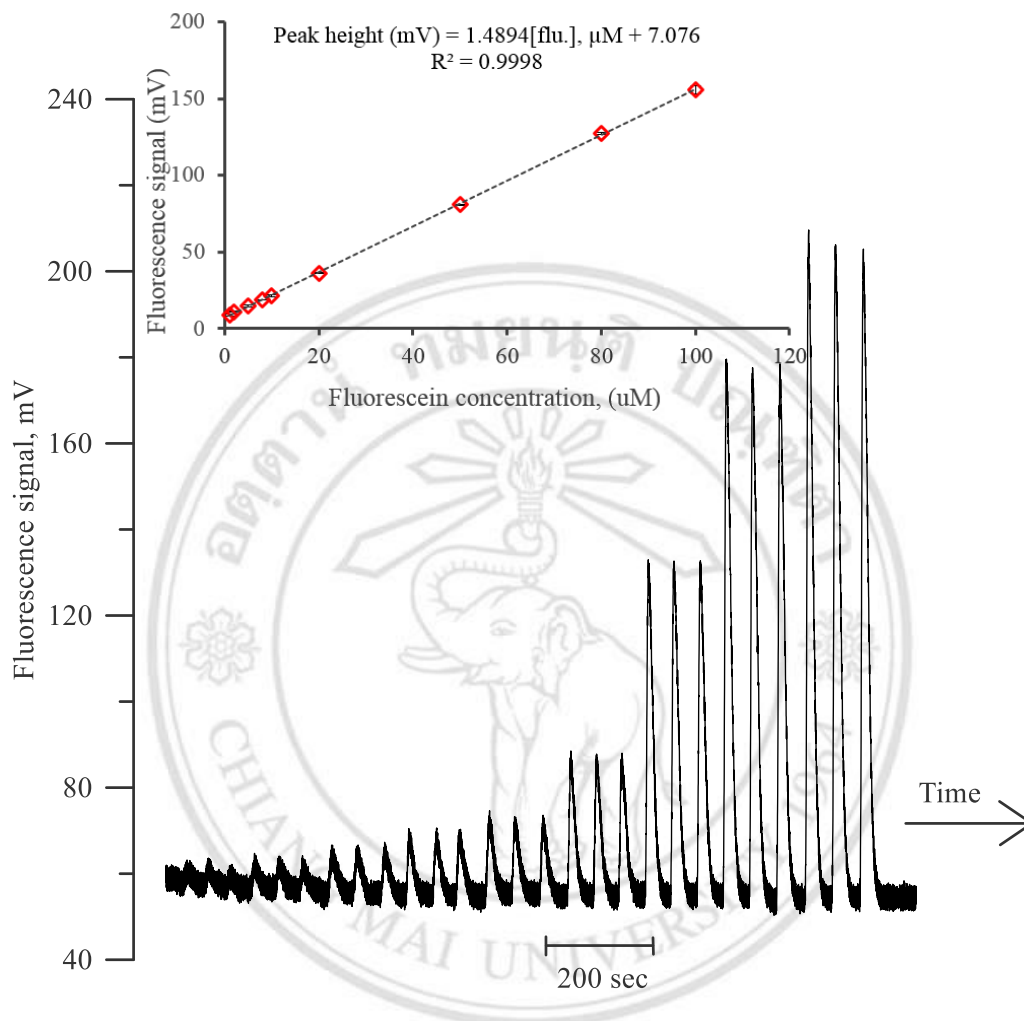


Figure 3.13 The FI-gram and linear calibration graph (inset) of 1-100 $\mu\text{mol L}^{-1}$ fluorescein injection in a single-FI system, (using UV-LED as the light source and an integrated photodiode and amplifier (OPT301) as the light sensor)

The OPA-sulfite reaction based ammonium determination is highly sensitive and selectivity which the flow setup was set as the single line FI/SI system without the GDU [40-41]. The 0.5 – 10 $\mu\text{mol L}^{-1}$ NH_4^+ was injected into the OPA reagent stream as demonstrated in schematic diagram of Figure 2.9. The reaction of ammonium-OPA-sulfite showed the slow reaction. Long mixing coil (200 cm) and water bath were set to promote the chemical reaction. In this study, the flow performance was affected by the length of mixing coil, temperature of reactor, flow rate of carrier, pH of OPA solution

and the injection volume. The flow conditions were similarly used as described in the previous study [17]. The FI-gram result and the linear relationship of calibration graph were shown in Figure 3.14.

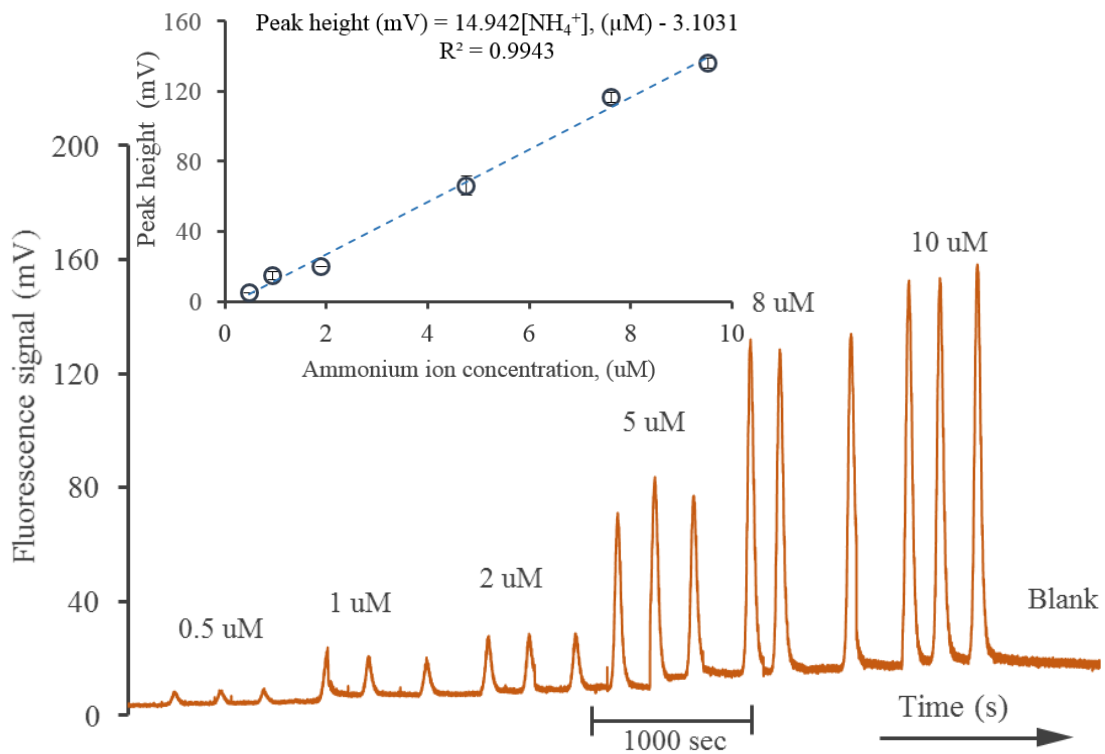


Figure 3.14 The FI-gram and linear calibration graph (inset) of 0.5-10 $\mu\text{mol L}^{-1}$ NH_4^+ in a single-FI system (67 μL injection volume with 200 cm length-mixing coil in 65°C water bath, 0.5 mL min^{-1} flow rate of OPA reagent as a carrier)

ลิขสิทธิ์มหาวิทยาลัยเชียงใหม่
Copyright © by Chiang Mai University
All rights reserved

3.2.2 The analytical performance for NH₄⁺ determination

The linear working range of NH₄⁺ detection was obtained in the range of 0.5-10 μmol L⁻¹ NH₄⁺ with the sample throughput of 15 injections h⁻¹. The limit of detection based on the lowest detection which is 0.5 μmol L⁻¹. The proposed fluorescence detector was highly sensitive technique which was applied to determine an ammonia in ambient air. In this study, the NH₄⁺ standard solution was spiked into the collected ammonia air sample to validate an accuracy of the proposed method. Four air samples were collected in 0.1 mol L⁻¹ H₂SO₄ as absorbing solution by using the air sampling system as illustrated in Figure 3.15. The recovery was obtained as shown in Table 3.5.

Table 3.5 The recovery of NH₄⁺ determination in air sample with a simple fluorescence detector

Sample	Dilution	NH ₄ ⁺ Added (μM)	NH ₄ ⁺ Found* (μM)	%Recovery
Air sample-1	50	0.0	3.20 ±0.3	
		0.95	4.21 ±0.1	106
		2.86	6.02 ±0.4	98.8
Air sample-2	20	0.0	2.69 ±0.1	
		0.95	3.70 ±0.1	106
		2.86	5.67 ±0.1	104
Air sample-3	50	0.0	1.01 ±0.0	
		0.95	1.61 ±0.1	62.2
		2.86	3.66 ±0.7	92.7
Air sample-4	20	0.0	1.96 ±0.1	
		0.95	2.88 ±0.3	96.1
		3.81	6.19 ±0.1	111

*The value is average ± SD (3 replicates)

3.2.3 Application for NH₄⁺ determination in air sample

The simple air sampling system was used to collect an ambient air from window in Science Complex Building (SCB2). The air sampling system comprises of absorbing solution chamber containing 0.1 mol L⁻¹ sulfuric acid solution, the NaOH solution bottle, rotameter, needle valve and air pump as illustrated in Figure 3.15. The flow rate of the air sampling system was controlled by using needle valve and was measured by using calibrated rotameter. The air samples were collected from different date and duration time with 65, 100 and 120 mL min⁻¹ flow rates and kept in a refrigerator at 4°C. The 10.0 mL of 0.1 mol L⁻¹ H₂SO₄ was used as absorbing solution. As a result, the concentration of ammonium in the absorbing solution can be converted to the concentration of ammonia in air in “ppbv” unit as shown in Table 3.6. The conversion factors involve the sampling flow rate, sampling duration and the absorbing solution volume.

Table 3.6 Concentration of NH₃ in air

Sample	Concentration of ammonia* (ppbv)
Air sample-1 ^a	26.7 ±2.4
Air sample-2 ^b	18.7 ±0.6
Air sample-3 ^a	8.4 ±0.3
Air sample-4 ^c	25.1 ±1.4

*The value is average ± SD (3 replicates)

^a100 minutes time sampling

^b120 minutes time sampling

^c65 minutes time sampling

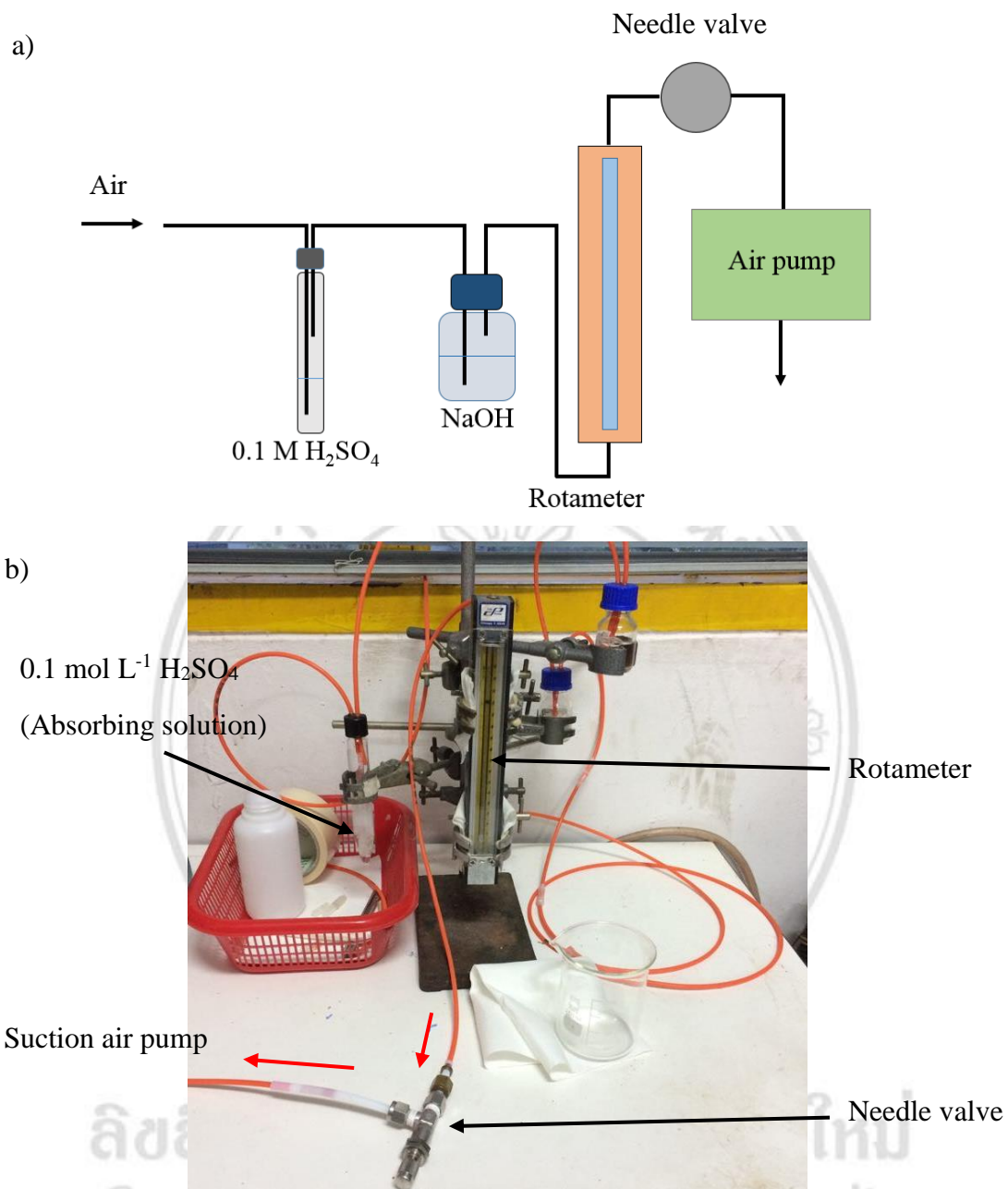


Figure 3.15 Schematic diagram (a) and photograph (b) of air sampling system (0.1 mol L^{-1} H_2SO_4 as an absorbing solution, 300 mL min^{-1} flow rate and 65-120 min sampling time)